Title
Thermal Energy Storage in Borehole Arrays Installed in Unsaturated Soils

ISBN
978-1-64368-032-3

Authors
Baser, Tugce
McCartney, John S
Ozdogan-Dolcek, Ayse

Publication Date
2019

DOI
10.3233/ASMGE190037

Peer reviewed

From Research to Applied Geotechnics
N.P. López-Acosta et al. (Eds.)

doi:10.3233/ASMGE190037

Thermal Energy Storage in Borehole Arrays Installed in Unsaturated Soils

Tugce BASER[a,1], John S. MCCARTNEY[b] and Ayse OZDOGAN-DOLCEK[c]
[a]*University of Illinois at Urbana-Champaign*
[b]*University of California, San Diego*
[c]*Balikesir University*

Abstract. In the last decades, much work has been performed to provide sustainable solutions for energy-related needs of society due to the increase in energy demands and concerns about warming of the climate. This includes using the subsurface as thermal energy sources such as in the Borehole Thermal Energy Storage (BTES) systems, an innovative approach to provide heating and cooling of the buildings through geothermal heat exchangers installed in the subsurface. This study focuses on the role of unsaturated soils on coupled thermo-hydraulic response of a BTES system, and specifically highlights how the coupled heat transfer and water flow processes and coupled thermo-hydraulic constitutive properties of soils may be exploited to optimize the performance of the BTES systems. A comprehensive study including characterization of constitutive properties of thermo-hydraulic properties and transient laboratory and field-scale responses of BTES systems, is performed. Then, the results from laboratory and full-scale field experiments are used to validate a three-dimensional finite element model to characterize heat transfer and heat storage within the BTES system. In addition, the economic and environmental impacts of the BTES systems are evaluated using a Life Cycle Assessment approach. The results indicate that the BTES systems can efficiently reduce energy consumption and CO_2 emissions that make these systems more attractive and environmentally friendly.

Keywords. BTES, heat transfer, renewable energy, unsaturated soils, LCA

1. Introduction

Borehole thermal energy storage (BTES) systems are an innovative approach, that allows to store heat collected from renewable sources in the subsurface that it can be used later for space or water heating. The BTES systems often use solar thermal panels generate heat during the day with a greater energy generation during summer months or heat recovered from waste water systems [1]. The BTES systems function in a similar way to Ground Source Heat Pumps (GHSP), where a carrier fluid is circulated through a closed-loop pipe network installed in vertical boreholes. Different from conventional GSHPs where a spacing of 2-3 m is used depending on the available space in the subsurface, the boreholes in a BTES system are spaced relatively close together (1-2 m) to concentrate heat within an array. BTES systems are proven to be an alternative to other systems as

[1] Tugce Baser, Assistant Professor, Dept. of Civil and Environmental Engineering, University of Illinois at Urbana-Champaign, 205 N. Mathews Ave, 2230C NCEL, Urbana IL 61801, USA; E-mail: tbaser@illinois.edu.

they use renewable energy resource such as solar energy rather than electricity and are space efficient as they are underground [2].

There are several successful BTES systems operating in Canada and Europe that use community-scale heat distribution systems. The Drake Landing BTES system in Canada provides 100% of the heat demand of 52 homes with an annual steady state efficiency of heat extraction over heat injection of 27% via solar thermal panels installed on garage roofs to an array of 144 boreholes in a 35 m-deep, 35-m wide grid [3]. Another successful SBTES system was installed in 2007 is in Braedstrup, Denmark that supplies heat from 18,000 m^2 of solar thermal panels to an array of 50 boreholes having a depth of 47-50 m installed across a 15 m-wide area [4]. This system provides 20% of the heat to 14000 homes. The most recent SBTES was installed in 2008 in Crailsheim, Germany involving of a series of 55 m-deep boreholes to form a 39000 m^3 subsurface storage volume. This system stores heat from 7410 m^2 of flat plate solar thermal collectors to provide heat for a school and 230 dwellings [5].

Although the experience from the community-scale systems at Drake Landing, Braedstrup, and Crailsheim indicates that BTES systems are functional and are sufficient to provide heating to communities at different scales, the simulation studies such as that of Catolico et al. [6] indicate that the hydrogeological setting is critical for optimizing the thermal energy storage. Therefore, this study focuses on providing a fundamental and applied understanding to the benefits of installing BTES systems in the vadose zone where the soil is unsaturated. The hypothesis of this research is based on to exploit the coupled thermal and hydraulic processes in the subsurface to take advantage of the multiple heat transfer mechanisms to increase the thermal storage capacity of the subsurface. To investigate the coupled heat transfer and water flow within borehole arrays, a full-scale BTES system was installed in University of California San Diego (UCSD) campus to monitor spatio-temporal temperature evolution during heating and cooling. The data from the experiments were used to calibrate and validate a three-dimensional finite-element-based numerical model to compare the amount of stored heat within the borehole array in different hydrological conditions.

The borehole thermal energy storage systems has become popular not only because of the increasing energy cost but also the climate change related issues such as increase in greenhouse gas (GHG) emissions with burning of fossil fuels. The BTES systems are proven to efficiently provide renewable energy and reduce the GHG emissions. However, the upfront and operational cost of these systems are still a consideration when choosing the most suitable heating and cooling system. USEIA [7] reported that the residential energy use is responsible for 30% of total annual energy consumption in the US and Heating Ventilating and Air Conditioning (HVAC) comprises 46% of the total residential energy consumption. Therefore, an efficient yet simple tool that considers cost and environmental impact can provide very useful information during the selection of the most suitable system to reduce the consumption. In this study, a life cycle analysis approach is used to perform life cycle cost and environmental impact analyses of the BTES system at UCSD using the actual data sets. The results are reported as a comparison to widely used traditional HVAC system, and GSHP system using the same assumptions and conditions.

2. Background

The major concern with BTES systems is the hydro-geological settings of the subsurface, because the soil type, amount of pore water, and in situ hydraulic gradients affect the thermo-hydraulic processes. Although the higher hydraulic gradients are favorable in GSHP systems, this is not true for BTES systems. Modeling the heat transfer in BTES systems installed in unsaturated soil profiles is complex because of the size of the system, geometry of the borehole array, and coupled constitutive relationships of thermal and hydraulic properties [8, 9]. Marcotte and Pasquier [10] numerically investigated the effect of the borehole configuration for the cases in which boreholes are connected in series, parallel, and mixed. They found that reported significantly lower inlet fluid temperatures for the parallel configuration than for the series configuration, indicating a larger heat transfer to the ground for this arrangement compared to the series configuration. Besides the geometrical configuration of the borehole heat exchangers there are other factors that affect the thermal response of a storage system, such as the subsurface temperature profile and ambient air temperature, degree of saturation profile of soil and the thermal properties. Other simulation efforts have recently been made using simplified numerical models that did not consider water vapor flow and phase change to understand the impacts of borehole array geometry, ground properties, heat injection magnitudes, and heat injection duration on the heat storage [11], characterize the behavior of borehole system behavior [12], understand the role of incorporating a thermal insulation layer [13]. Başer et al. [13] evaluated the importance of understanding the impacts of different modes of heat transfer in SBTES systems in the vadose zone and found that it was critical to consider water vapor flow and phase change. Başer et al. [14] investigated the effect of the ambient air temperature fluctuation on the heat storage systems and found that including ambient air temperature in the modeling efforts is worthwhile because ambient air temperature can penetrate up to 9 m from the surface. On the other hand, Nguyen et al. [15] showed that seasonal temperature variation of the subsurface increases the outlet fluid temperature causing a decrease in the heat transfer rate into the ground. Further, they found that burying boreholes at the certain depth from the surface (1-2 m) was not sufficient to hinder the ambient air temperature effects on the ground temperature near the surface. Thus, it is important to utilize validated tools to optimize these systems because of the economic concerns.

3. Field Installation

A full-scale BTES system was installed at the Englekirk Structural Engineering Center on the University of California San Diego campus. The system was sited in a 1 m of silty sand underlain by conglomerate bedrock, with a groundwater table more than 30 m deep. The BTES system consists of a network of 25 mm-diameter high density polyethylene (HDPE) U-shape heat exchanger tubing installed within 15 m deep, thirteen of boreholes in a hexagonal array with a spacing of 1.5 m as shown in Figure 1. Three additional boreholes (two within and one outside of the array) were drilled to include temperature sensors at different depths. Although the number of boreholes is much smaller than those incorporated into the district-scale heating systems mentioned above, it provides an important data point in the scaling of BTES systems for different sizes of communities. More details on the installation procedures can be found in Baser and McCartney [8].

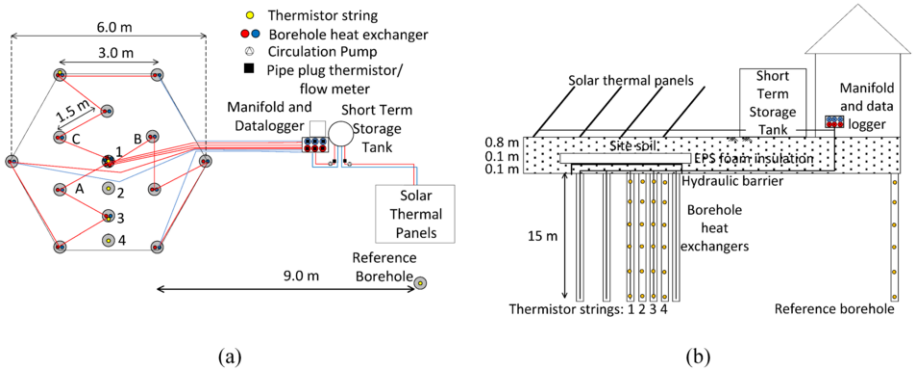

Figure 1. UCSD BTES system: (a) Plan view, (b) Elevation view of BTES system.

4. Numerical Model

Simulation of coupled heat transfer and liquid water and water vapor in unsaturated soils requires solving for four main variables: temperature, pore water pressure, pore total gas pressure, and vapor concentration using two phase flow model in which temperature and vapor pressure gradients are implemented. Governing equations for heat transfer and water flow in a continuum are presented in Table 1 (Eqs. (1) through (6)). The main assumptions of the model are: (a) soil framework is homogeneous, isotropic, and non-deformable; (b) fluid phases are immiscible; (c) hysteresis in the constitutive relationships is not considered.

Table 1. Constitutive models used in the numerical analyses.

Equation
Governing equation for liquid water flow: $$nS_{rw}\frac{\partial \rho_w}{\partial t}+n\rho_w\frac{dS_{rw}}{dP_c}\frac{\partial P_c}{\partial t}+\nabla\cdot\left[\rho_w\left(-\frac{k_{rw}\kappa}{\mu_w}\right)\nabla\left(P_w+\rho_w gz\right)\right]=-R_{gw} \quad (1)$$ n=porosity (m^3/m^3), S_{rw}=degree of water saturation (m^3/m^3), ρ_w=temperature-dependent density of water (kg/m^3) [16], t=time(s), $P_c=P_w-P_g$=capillary pressure (Pa), P_w=pore water pressure (Pa), P_g=pore gas pressure (Pa), k_{rw}=relative permeability function for water (m/s); κ=intrinsic permeability (m^2); μ_w=temperature-dependent water dynamic viscosity (kg/(ms)) [17], g=acceleration due to gravity (m/s^2) R_{gw}=Phase change rate (kg/m^3s) [18, 19]
Governing equation for total gas flow: $$nS_{rg}\frac{\partial \rho_g}{\partial t}+n\rho_g\frac{dS_{rg}}{dP_c}\frac{\partial P_c}{\partial t}+\nabla\cdot\left[\rho_g\left(-\frac{k_{rg}\kappa}{\mu_g}\right)\nabla\left(P_g+\rho_g gz\right)\right]=R_{gw} \quad (2)$$ S_{rg}=degree of gas saturation (m^3/m^3), ρ_g=temperature-dependent density of gas (kg/m^3) [20], k_{rg}=relative permeability function for gas (m/s); μ_g=temperature-dependent gas dynamic viscosity (kg/(ms)) [18, 19]

Table 1. (*continued*) Constitutive models used in the numerical analyses.

Equation
Water vapor mass balance equation: $$n\frac{\partial\left(\rho_g S_{rg} w_v\right)}{\partial t} + \nabla\cdot\left(\rho_g u_g w_v - D_e \rho_g \nabla w_v\right) = R_{gw} \quad (3)$$ $D_e=D_v\tau$=effective diffusion coefficient (m^2/s), D_v=diffusion coefficient of water vapor in air (m^2/s) [21], w_v=mass fraction of water vapor in the gas phase (kg/kg), $\tau=n^{1/3}S_{rg}^{7/3}\eta$=tortuosity [22, 20]
Enhancement factor for vapor diffusion, η: $$\eta = a + 3S_{rw} - (a-1)\exp\left\{-\left[\left(1+\frac{2.6}{\sqrt{f_c}}\right)S_{rw}\right]^3\right\} \quad (4)$$ a=empirical fitting parameter, f_c= clay content [23]
Nonequilibrium gas phase change rate, R_{gw}: $$R_{gw} = \left(\frac{bS_{rw}RT}{M_w}\right)\left(\rho_{veq} - \rho_v\right) \quad (5)$$ b=empirical fitting parameter (s/m^2), R=universal gas constant (J/molK), ρ_{veq}=equilibrium vapor density (kg/m^3) [21], T=Temperature (K), ρ_v=vapor density (kg/m^3), M_w=molecular weight of water (kg/mol) [24, 19]
Heat transfer energy balance: $$\left(\rho C_p\right)\frac{\partial T}{\partial t} + \nabla.\left(\left(\rho_w C_{pw}\right)u_w T + \left(\rho_g C_{pg}\right)u_g T - \left(\lambda\nabla T\right)\right) = -LR_{gw} + Q \quad (6)$$ ρ=total density of soil (kg/m^3), C_p=specific heat of soil (J/kgK), C_{pw}=specific heat capacity of water (J/kgK), C_{pg}=specific heat capacity of gas (J/kgK), λ=thermal conductivity (W/mK), L=latent heat due to phase change (J/kg), u_w=water velocity (m/s), u_g=gas velocity (m/s), Q=heat source (W/m^3) [25,19]

As can be seen in Table 1, the governing equations don't include the constitutive relationships of thermo-hydraulic properties of unsaturated soils. To solve the sets of coupled equations, the constitutive equations were used to consider the effect of temperature on density, viscosity, surface tension, SWRC, and change in thermal conductivity and volumetric heat capacity with changing degree of saturation.

Table 2. Constitutive models used in the numerical analyses.

Equation
Soil Water Retention Curve (SWRC): $$S_{rw} = S_{rw,res} + \left(1 - S_{rw,res}\right)\left[\frac{1}{1+\left(\alpha_{vG} P_c(T)\right)^{N_{vG}}}\right]^{1-1/N_{vG}} \quad (7)$$ where $S_{rw,res}$ is the residual degree of saturation to water, α_{vG} and NvG are parameters representing the air entry pressure and the pore size distribution, respectively, and Pc(T) is the temperature-corrected capillary pressure according to the model of Grant and Salehzadeh [26, 27]
Hydraulic Conductivity Function (HCF): $$k_{rw} = \sqrt{\left(\frac{S_{rw} - S_{rw,res}}{1 - S_{rw,res}}\right)}\left[1 - \left(1 - \left(\frac{S_{rw} - S_{rw,res}}{1 - S_{rw,res}}\right)^{1/(1-1/N_{vG})}\right)^{1-1/N_{vG}}\right]^2 \quad (8)$$ where α_{vG} and NvG are the same parameters as in Eq. (7) [28, 29]
Thermal Conductivity Function (TCF): $$\frac{\lambda - \lambda_{\text{dry}}}{\lambda_{\text{sat}} - \lambda_{\text{dry}}} = 1 - \left[1 + \left(\frac{S_e}{S_{\text{f}}}\right)^m\right]^{1/m-1} \quad (9)$$ where λ_{dry} and λ_{sat} are the thermal conductivities of dry and saturated soil specimens, respectively, S_e is the effective saturation, S_f is the effective saturation at which the funicular regime is onset, and m is defined as the pore fluid network connectivity parameter for thermal conductivity [29]
Volumetric Heat Capacity Function (VHCF): $$\frac{C_v - C_{v\,\text{dry}}}{C_{v\,\text{sat}} - C_{v\,\text{dry}}} = 1 - \left[1 + \left(\frac{S_e}{S_{\text{f}}}\right)^m\right]^{1/m-1} \quad (10)$$ where C_{vdry} and C_{vsat} are the volumetric heat capacities of dry and saturated soil, respectively, and are similarly treated as fitting parameters, and S_f and *m* are the same parameters as in Eq. (9) [14]

4.1. Calibration

To simulate the BTES system, first the numerical model needs to be calibrated for site-specific soil properties. The reconstituted site-soil was compacted to a dry density of 1650 kg/cm^3 at an initial degree of saturation of 0.49. The thermo-hydraulic constitutive

relationships were determined using a transient water release and imbibition method (TRIM) of Wayllace and Lu [30] that included the measurement of the thermal conductivity and volumetric specific heat capacity described by Lu and Dong [29]. The soil water retention curve (SWRC), hydraulic conductivity function (HCF), thermal conductivity function (TCF), and volumetric heat capacity function (VHCF) were obtained using equations given in Table 2. The SWRC and HCF along with relevant parameters are shown in Figure 2(a), while the TCF and VHCF are shown in Figure 2(b).

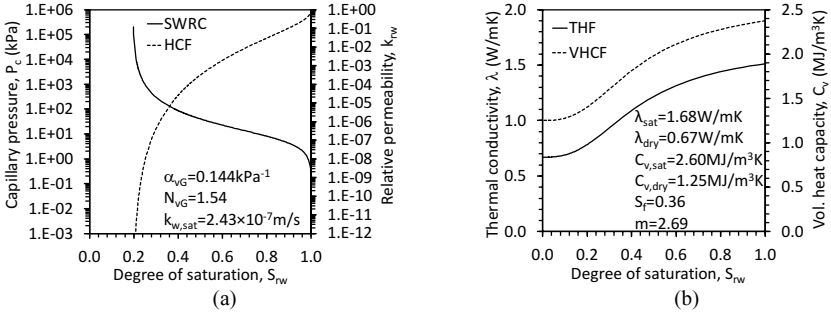

Figure 2. Coupled material properties (a) SWRC and HCF; (b) TCF and HCF.

A laboratory heating experiment was performed to characterize the thermo-hydraulic processes through site-soil as well as to provide a data set to calibrate the numerical model for empirical parameters *a* and *b*. A heating element was used to apply constant temperature for thirty-six hours at the bottom of the soil specimen that placed in a modified standard compaction mold by Iezonni and McCartney [31], which allows to include dielectric sensors in the middle of the mold. During the experiments, temporal evolution of temperature and degree of saturation were recorded. Then, the sets of coupled equations were solved using COMSOL Multiphysics v5.3 using identical initial and boundary conditions to the laboratory experiment to compare the numerical results with data collected from the experiment. The comparisons of time series are given in Figures 3(a) and 3(b). The numerical model predicted temperature and degree of saturation for *a* and *b* values of 20 and 2x10^{-7} s/m^2, respectively.

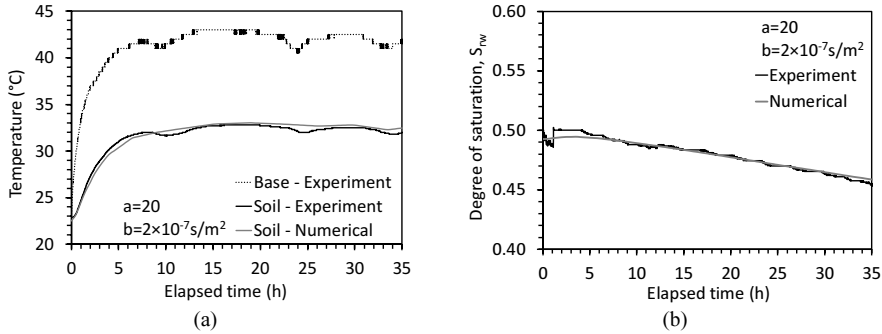

Figure 3. Comparisons of time series for experimental and numerical results: (a) Temperature; (b) Degree of saturation.

4.2. Simulations

The calibrated model was used to simulate the thermo-hydraulic response of unsaturated soils as well as the transient behavior of full-scale BTES system demonstration experiment. A plan view of the BTES system showing the connections between the borehole array, and the simulated domain are given in Figures 4(a) and 4(b). As the hexagonal borehole array is symmetrical, a quarter section was simulated as shown in Figure 4. This figure also includes the labels used to name the thirteen boreholes that include heat exchangers (boreholes A through M) and the four boreholes that include thermistor strings (T-1 to T-4). The model domain is 15 m x 15 m in plan and has a depth of 20 m and includes 5 borehole heat exchangers. The size of the domain was selected such that the heat exchangers would not affect the temperatures at the boundaries for the heat injection period under investigation. This was confirmed by ensuring that the temperature at the boundary of the array remained similar to the temperatures from the reference borehole at different depths.

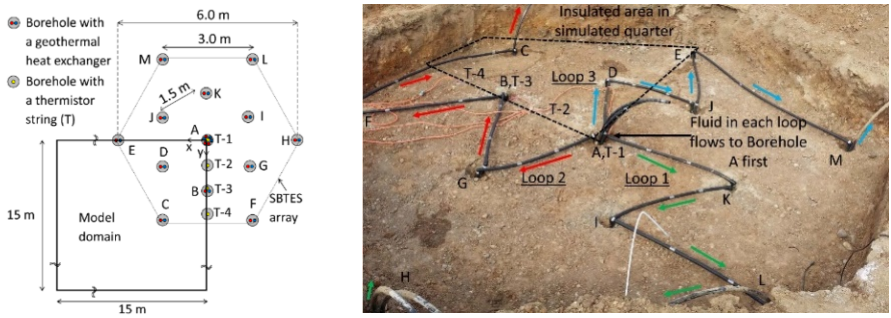

(a) (b)

Figure 4. Simulated model domain: (a) Plan view; (b) Picture.

The plan views of the model domain shown in Figures 5(a) and 5(b) highlight the thermal and hydraulic boundary and initial conditions, respectively. The initial temperature profile was obtained from the ground temperature distribution measured by the reference borehole at the initiation of the heat injection period on April 29th, 2016. To define the initial degree of saturation profile, hydrostatic conditions were assumed. Although the water table was not encountered in the previous geotechnical site investigation which was performed in 2003, San Diego County Water Authority reported that the ground water depth ranges in depth from 14 to 24 m in the area. Accordingly, the water table was fixed at a depth of 20 m from the surface (at the base of the domain) throughout the simulations. Based on the hydrostatic profile shown in Figure 6(b), the initial degree of saturation along most of the length of the heat exchangers was approximately 0.22 which corresponds to residual saturation conditions. Near the bottom of the heat exchangers, the initial degree of saturation increases up to 0.49 due to the proximity of the water table.

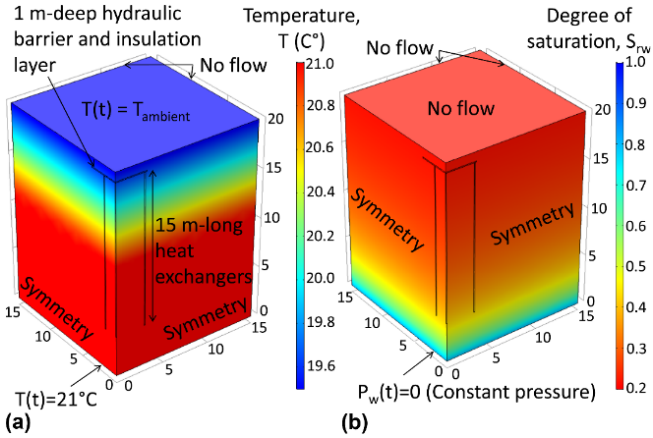

Figure 5. Initial and boundary conditions on the quarter domain model for a field-scale geothermal heat exchanger (JC is mass flux, distances in meters): (a) Thermal; (b) Hydraulic.

As could be expected from the large fluctuations in the heat transfer rate into the geothermal heat exchanger loops due to the variability in the solar thermal heat transfer rate, the temperature at the locations of the borehole heat exchangers are expected to experience significant changes in temperature each day. A comparison between the temperatures at the location of thermistor string T-2 shown in Figure 6. The temperature at the location of thermistor string T-2 depends on overlapping effects of borehole heat exchangers A and B, and heat transfer from these boreholes damps out the daily fluctuations. A good match in the trends and magnitudes at the different depths was observed during both the heat injection and ambient cooling periods, with only a slight underestimation of the temperature at depths of 16.00 m and 1.82 m. The measured temperature values during the heating injection period ranged from 29.5 °C near the bottom of the array to 34.2 °C near the top of the array. The greater increases in measured and simulated temperatures near the surface of the array may be due to greater heat transfer in initially dryer soils due to greater water vapor diffusion and latent heat transfer as well as buoyancy-driven upward movement of water vapor, both of which were observed by Baser et al. [9] in the simulation of a single geothermal heat exchanger.

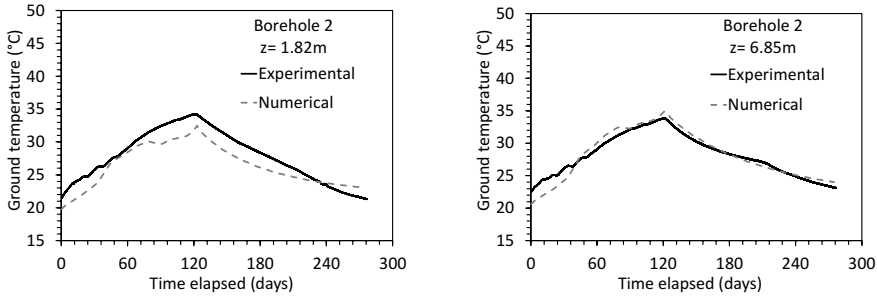

Figure 6. Predicted and measured temperature time series from thermistor string T-2 for different depths (z): (a) 16.00m; (b) 14.78m; (c) 12.95m; (d) 9.29m; (e) 6.85m; (f) 1.82m.

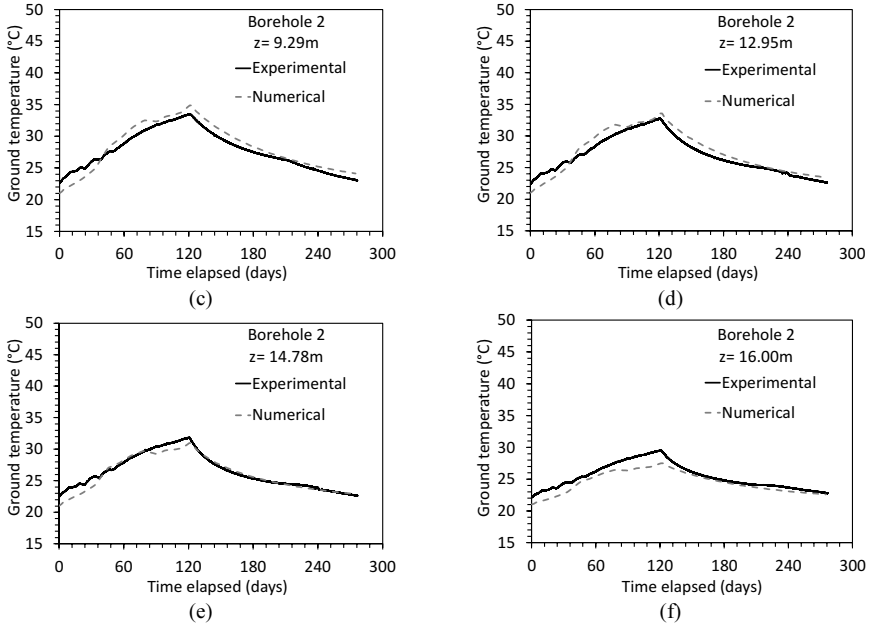

Figure 6. (*continued*) Predicted and measured temperature time series from thermistor string T-2 for different depths (z): (a) 16.00m; (b) 14.78m; (c) 12.95m; (d) 9.29m; (e) 6.85m; (f) 1.82m.

Radial profiles of temperatures at the end of the heat injection period from the numerical model and the field measurements are shown in Figure 7(a) for the depths that thermistors were installed. As seen in Figure 7(a), simulated temperatures were in good agreement, especially at depths of 14.78 and 1.82 m. This figure also includes the ground temperatures from the reference borehole which was at a radial distance of 10 m from the center of the borehole array to further validate the numerical model. The shapes of the radial profiles are similar to those interpreted from the field measurements, although the maximum temperatures at the locations of thermistor strings 1 and 3 due to the daily fluctuations in heat transfer rate were not captured. Radial distributions in temperature at the end of the ambient cooling period indicate that some heat (a maximum difference in temperature of 4 °C from the initial value of 21 °C) is still retained within the array after 5 months of ambient cooling as shown in Figure 7(b).

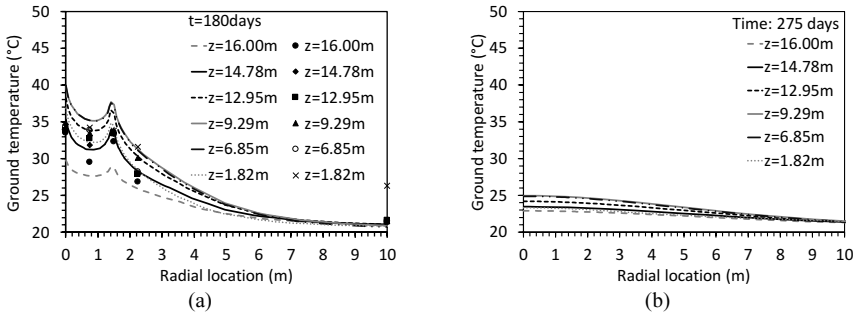

Figure 7. Radial temperature profiles at different depths (z): (a) At the end of heating; (b) After 5 months of ambient cooling.

4.3. Heat Storage

To quantify the heat stored in within the BTES system, a volume of storage is defined as the volume of borehole array assuming that any heat transferred across the outer boundaries are lost to validate hypothesis of this research. Two additional simulations were performed using the same geometry and initial and boundary conditions to compare three different hydrologic settings: (1) unsaturated, (2) saturated, and (3) dry. Then, the heat fluxes within the volume of storage were integrated over volume to calculate the power (W) and integrated over time to calculate the amount of thermal energy (GJ) retained within the same volume of storage. As seen in Figure 8, approximately 30 GJ which corresponds to the 77% of the total injected heat retained within the storage in the case of unsaturated soil while this amount was the least for saturated condition even hydrostatic conditions were assumed in the simulations. The % values in the figure indicate the heat transferred across the outer boundary of the array.

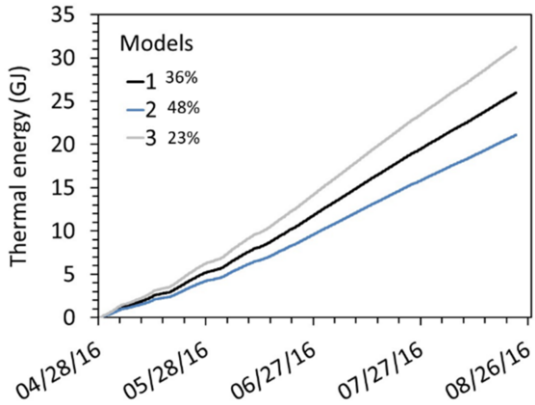

Figure 8. Comparisons of heat storage for different hydrological conditions.

5. Life Cycle Analysis of BTES

5.1. Procedure

In this study the BTES system where the heat is collected through solar panels as indicated earlier, is assessed in terms of its sustainability through its life cycle. Specifically, to investigate whether the BTES systems have more economic and environmental benefits compared to natural gas air conditioning (NGAC) and GSHP systems, a Life Cycle Assessment (LCA) approach is used to compare the life cycle cost (LLC) and environmental impact (e.g. CO_2 emission). Because the data from BTES system in San Diego, CA only includes one-year initial storage cycle, the energy cost during operation of each unit is considered for only the transient heating period.

A large data inventory is needed for a full LCA to include all the stages of a product's life from raw material extraction through materials processing, manufacture, distribution, use, repair and maintenance, and disposal/or recycling. There are various computer tools that are capable of performing the LCA of residential heating and cooling systems. Such tools include SimaPro [33, 34], Gabi5 Software [35], and RETScreen [36]. One of the

most critical implementations of LCA is the determination of the environmental impact of energy sources or life cycle energy assessment (LCEA). Considering increasing energy demand and the concern for global warming potential (GWP) is an important characterization category of LC [37]. GWP is considered a midpoint category, typically quantified by GHG emissions using units of CO_2 equivalent (CO_{2eq}). Although the predominant atmospheric GHG is CO_2 (84%), methane, nitrous oxide, carbon monoxide, and fluorinated gases contribute significantly [38]. During the analyses, the CO_2 equivalence value of each GHG can be calculated and it depends on the methods used.

In this study, present value method (PV) is used to conduct LLC analysis of BTES systems. This method was used in various projects [33, 39] and it provides relatively a quick approach that converts the future value of system into the present value by considering the discount rate and the time value as follows:

$$LCC = IC + \sum_{i=0}^{n} \frac{ECi}{(1+r)^i} \tag{11}$$

where IC is investment cost, EC is the annual energy, r is the real discount rate, n is the period of life-cycle analysis. IC includes purchase price of main equipment, construction, and installation cost. The discount rate, r was assumed 5% as suggested by The World Bank [40]. The rate of increase of energy cost (inflation) was set to 3%. Annual EC is calculated based on energy sources utilized in each SBTES, GSHP and NGAC heating and cooling units. Since the BTES system is operating to store heat and use it later for the heating purpose only, the energy cost used for the space heating is considered in this study.

GSHP systems require energy inputs during the use phase of electricity used by the heat exchangers and circulation pumps. For the purposes of this study, GSHP energy use is estimated with a theoretical model based on climate and building load for the state of California. This model, adapted from the study by Fredin [41], divides the building load into heating and cooling consumption. According to the model, there are two annual electricity input for a GSHP system for heating season calculated using Eqs. (12a) and (12b) as follows:

$$\mathrm{GSHP}_{\mathrm{Heating[kWh]}} = \frac{\text{Heating Load}\left[\frac{\mathrm{BTU}}{\mathrm{hr}}\right] \times \mathrm{HDD[hr]}}{\mathrm{COP} \times 3145\left[\frac{\mathrm{BTU}}{\mathrm{kWh}}\right]} \tag{12a}$$

$$\text{GSHP Circulating Pump}_{\mathrm{Heating[kWh]}} = \frac{\text{Pump Power[W]} \times \mathrm{HDD[hr]}}{\text{Motor Efficiency[\%]} \times 1000\left[\frac{\mathrm{W}}{\mathrm{kW}}\right]} \tag{12b}$$

where HDD is the heating degree days and COP is the coefficient of performance that is ratio of useful energy, which is a system's output energy to its input energy use to run the GSHP system. Typical GCHPs have a COP of 3 to 4 [34], the COP for CA region is assumed as 3.5 [42]. Heating loads (26.2 kBtu/hr) and heating degree days (2948 hr) are used for a typical residential house of 2000 sq. (186 m^2) from previous study done by Fredin [41]. Motor efficiency is taken as 88% [43] and combined circulating pump power is 50 W.

Another input in this approach is the energy use of a natural gas furnace during the heating season that are used as the baseline to quantify the energy savings and environmental impact. The NGAC uses natural gas for heating and electricity for both air conditioning and to run the fan in the furnace. Assuming an equal lifetime and equal heating loads for a natural gas system, the electricity and natural gas consumption are calculated using Eqs. (13a) and (13b) as follows:

$$NGAC_{\text{Heating [kWh Elec.]}} = \frac{\text{Fan Power[W]} \times \text{HDD[hr]}}{\text{Motor Efficiency[\%]} \times 1000 \left[\frac{\text{W}}{\text{kW}}\right]} \tag{13a}$$

$$\text{NGAC}_{\text{Heating [kWh NG]}} = \frac{\text{Heating Load} \left[\frac{\text{BTU}}{\text{hr}}\right] \times \text{HDD[hr]}}{\text{AFUE} \times 3145 \left[\frac{\text{BTU}}{\text{kWh}}\right]} \tag{13b}$$

where EER is the energy efficient ratio taken to be 14.4, AFUE is the annual fuel utilization efficiency of natural gas assumed a mid-efficiency value of 80% [44], motor efficiency 85% and fan power ⅓ HP (249 W). For BTES, energy is only consumed through operation of circulating pump, in which fluid is circulated through solar panels and array of borehole heat exchangers. Both solar and ground loops use electricity to operate the circulation pump during heat injection into the ground. Energy consumption of solar circulation pump with a power capacity of 90 W and an additional pump with a power supply of 249 W were calculated using Eq. (3).

5.2. Eco-efficiency

Solving Eq. (11) through 13, the total annual energy cost during operation is calculated and then extrapolated to a 25-year lifetime to define LCC for the operational impact of the BTES, GSHP, and NGAC systems. If energy sources for electricity use of these three systems are assumed to be natural gases, U.S. Energy Information Administration reports that the amount of CO_2 emissions is 53.07 kg/ million Btu (5.52 kg/kWh). The energy consumption of BTES, GSHP, and NGAC systems and CO_2 emissions in metric ton per kWh are calculated and the results are given in Figure 9. According to the results, the 25-year operational cost of the BTES system was only $2,000, while this value was $28,000 for the NGAC system. The main operational cost of the GSHP was the heat pump and the natural gas purchase for the NGAC system, respectively. The operational costs of the systems reflect to CO_2 emissions with the same trend, NGAC systems emits largest amount of CO_2 and while the BTES emits the least CO_2 with an amount of 250 ton/kWh which is 83% less than GSHP and 96% than those of NGAC system.

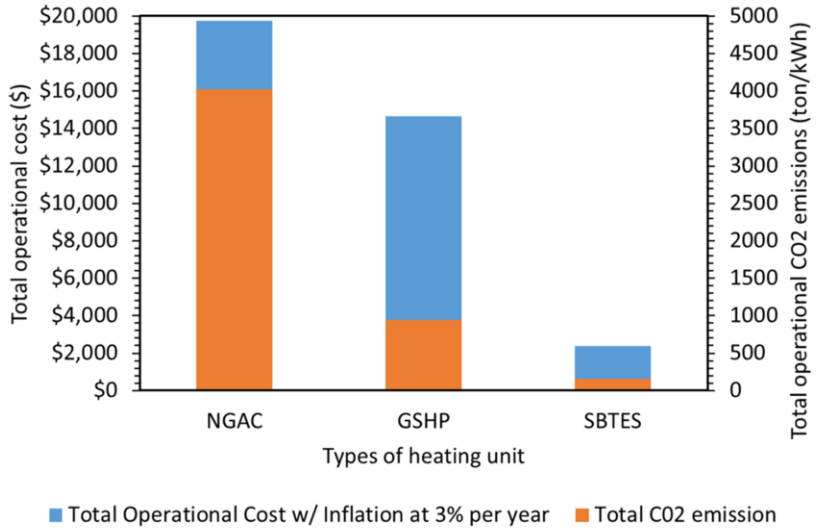

Figure 9. Life cycle cost impact of BTES, GSHP, and NGAC for 25-year of operation.

While the results from only 25-year operation was promising for BTES systems, an additional LCC analysis is needed to quantify the investment cost of all three systems. The LCC results of the BTES, GSHP, and NGAC systems are shown in Figure 10. The LCC of the BTES system was $32,000 while this value for GSHP and NGAC systems were $23,800 and $24,255, respectively. One interesting observation from the Figure 10 is the similar LCC of GSHP and NGAC systems.

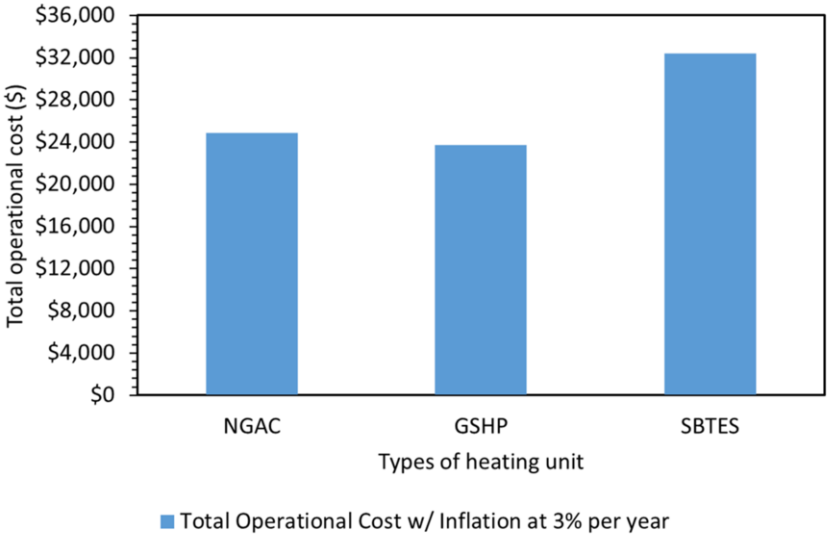

Figure 10. Life cycle cost of three different heating units (investment + operational).

6. Conclusions

This study focused on understanding the heat storage characteristics of borehole thermal energy storage (BTES) systems installed in the vadose zone. A full-scale, fully instrumented BTES system was installed in an unsaturated soil profile in San Diego, CA and subjected to a heating and cooling experiment to monitor the thermal response of the borehole array.

A calibrated and validated three-dimensional numerical model based on finite element method was used to calculate the retained heat within the borehole array to represent three different hydrologic settings: unsaturated, saturated, and dry soil profiles. It was seen that in the case of unsaturated soil, the highest amount of heat retained after the cooling period.

In addition to physics-based modeling of the BTES system, a life cycle assessment approach, eco-efficiency analysis was used to quantify the life cycle cost and environmental impact of the BTES system, and the results were compared with traditional heating and cooling systems such as ground source heat pump (GSHP) and natural gas air conditioning systems (NGAC). The results revealed that he BTES had the highest life cycle cost due to its higher investment cost compared to GSHP and NGAC, but it is more effective in terms of operational cost that will likely pay the capital cost in a short period of time. When high effective operational cost of the BTES is considered, these systems could be the best alternative in a region with moderate climate.

References

[1] McCartney, J.S., Ge, S., Reed, A., Lu, N., and Smits, K. (2013). "Soil-borehole thermal energy storage systems for district heating." Proceedings of the European Geothermal Congress 2013. Pisa. Jun. 3-7. pp. 1-10.

[2] Baser, T. and McCartney, J.S. (2015a). "Development of a full-scale soil-borehole thermal energy storage system." Proc. Int. Foundation Conference and Equipment Exposition (IFCEE 2015). ASCE, Reston, VA. pp. 1608-1617.

[3] Sibbitt, B., McClenahan, D., Djebbar, R., Thornton, J., Wong, B., Carriere, J., Kokko, J. (2012). "The performance of a high solar fraction seasonal storage district heating system - Five years of operation." Energy Procedia. 30, 856-865.

[4] Bjoern, H. (2013). "Borehole thermal energy storage in combination with district heating." EGC 2013. Pisa. June 3-7. 1-13.

[5] Nussbicker-Lux, J. (2012). "The BTES project in Crailsheim (Germany) – Monitoring results." Proc. 12th Int. Conf. on Energy Storage – Innostock. IEA Press, Paris. 1-10.

[6] Catolico, N., Ge, S., and McCartney, J.S. (2016). "Numerical modeling of a soil-borehole thermal energy storage system." Vadose Zone Hydrology. 1-17.doi:10.2136/vzj2015.05.0078.

[7] U.S.EIA. (2009). Household Energy Use in California.

[8] Başer, T. and McCartney, J.S. (2018). "Transient performance evaluation of solar thermal energy storage in a geothermal borehole array". Renewable Energy, https://doi.org/10.1016/j.renene.2018.11.012

[9] Baser, T., Dong, Y., Moradi, A.M., Lu, N., Smits, K., Ge, S., Tartakovsky, D., and McCartney, J.S. (2018). "Role of water vapor diffusion and nonequilibrium phase change in thermal energy storage systems in the vadose zone." Journal of Geotechnical and Geoenvironmental Engineering. https://doi.org/10.1061/(ASCE)GT.1943-5606.0001910

[10] Marcotte, D. and Pasquier, P. (2014). "Unit-response function for ground heat exchanger with parallel, series or mixed borehole arrangement." Renewable Energy. 68, 14–24.

[11] Başer, T. and McCartney, J.S. (2015b). "Thermal energy storage in borehole arrays." Symposium on Energy Geotechnics. Barcelona. Jun. 2-4. pp. 1-2.

[12] Baser, T., Lu, N., and McCartney, J.S. (2016a). "Operational response of a soil-borehole thermal energy storage system." ASCE Journal of Geotechnical and Geoenvironmental Engineering. 04015097-1-12. 10.1061/(ASCE)GT.1943-5606.0001432.
[13] Baser, T., Dong, Y., Lu, N., and McCartney, J.S. (2016d). "Role of considering non-constant soil thermal parameters in the simulation of geothermal heat storage systems in the vadose zone". Proceedings. 8th Asian Young Geotechnical Engineers Conference 2016 (AYGEC 2016). Kazakh Geotechnical Society. Astana. pp. 1-6.
[14] Baser, T., McCartney, J.S., Moradi, A., Smits, K., and Lu, N. (2016b). "Effect of a thermo-hydraulic insulating layer on the long-term response of soil-borehole thermal energy storage systems". GeoChicago 2016: Sustainability, Energy and the Geoenvironment. Chicago. Aug. 14-18. ASCE, Reston, VA. pp. 125-134.
[15] Nguyen, A., Pasquier, P., and Marcotte, D. (2017). "Borehole thermal energy storage systems under the influence of groundwater flow and time-varying surface temperature." Geothermics. 66, 110-118.
[16] Hillel, D. (1980). Fundamental of Soil Physics. Academic, San Diego, CA.
[17] Lide, D. R. (2001). Handbook of chemistry and physics. Boca Raton, FL: CRC Pres.
[18] Bear, J. (1972). Dynamics of Fluids in Porous Media. Dover, Mineola, N.Y., 764.
[19] Moradi, A. M., Smits, K., N. Lu, and J. S. McCartney (2016). "3-D experimental and numerical investigation of heat transfer in unsaturated soil with an application to soil borehole thermal energy storage (SBTES) systems." Vadose Zone J. 15 (10): 1–17. https://doi.org/10.2136/vzj2016.03.0027
[20] Smits, K.M., Cihan, A., Sakaki, S., and Illangasekare, T.H. (2011). "Evaporation from soils under thermal boundary conditions: Experimental and modeling investigation to compare equilibrium- and nonequilibrium-based approaches." Water Resources Research. 47, W05540, doi:10.1029/2010WR009533.
[21] Campbell, G.S. (1985). Soil Physics with BASIC: Transport Models for Soil–Plant Systems. Elsevier, New York.
[22] Millington, R.J., and Quirk, J.M. (1961). "Permeability of porous solids." Trans. Faraday Soc. 57, 1200–1207.
[23] Cass, A., Campbell, G.S., and Jones. T.L. (1984.) "Enhancement of thermal water vapor diffusion in soil." Soil Science Society of America. 48(1), 25–32.
[24] Bixler, N.E. (1985). NORIA: "A Finite Element Computer Program for Analyzing Water, Vapor, Air and Energy Transport in Porous Media." SAND84-2057, Sandia National Laboratories, Albuquerque, NM.
[25] Whitaker, S. (1977). "Simultaneous heat, mass and momentum transfer in porous media: A theory of drying porous media." Adv. Heat Transf. 13: 119–203. https://doi.org/10.1016/S0065-2717(08)70223-5.
[26] Grant, S.A. and Salehzadeh, A. (1996). Calculations of temperature effects on wetting coefficients of porous solids and their capillary pressure functions. Water Resources Res. 32(2), 261-279.
[27] van Genuchten, M.T. (1980). "A closed-form equation for predicting the hydraulic conductivity of unsaturated soils." Soil Sci. Soc. Am. J. 44(5), 892–898.
[28] Mualem, Y. (1970). The Form of the interface in steady flow in a stratified porous medium (Hebrew). Thesis for M.Sc., Technion, Israel Institute of Technology, Haifa, Israel, 1970.
[29] Lu, N. and Dong, Y. (2015). "A closed form equation for thermal conductivity of unsaturated soils at room temperature." Journal of Geotechnical and Geoenvironmental Engineering. 141(6), 04015016.
[30] Wayllace, A. and Lu, N. (2012). "A transient water release and imbibitions method for rapidly measuring wetting and drying soil water retention and hydraulic conductivity functions." Geotechnical Testing Journal. 35(1), 103-117.
[31] Iezzoni, H. M. and McCartney, J.S. (2016). "Calibration of Capacitance Sensors for Compacted Silt in Non-Isothermal Applications." Geotechnical Testing Journal, Vol. 39(2), 169-180.
[32] McCartney, J.S. and Başer, T., (2017). "Role of coupled process in thermal energy storage inthe vadose zone". ISSMGE CPEG2 2017, September 6-7, Leeds, UK.
[33] Aquino, A., Bonamente, E., Rinaldi, S., & Nicolini, A. (2017). Life cycle assessment of a ground-source heat pump including an upstream thermal storage Hydrate-based biogas upgrading and integration with other energy processes View project. Perugia, Italy April 6-7, 2017: 17th CIRIAF National Congress Sustainable Development, Human Health and Environmental Protection. Retrieved from https://www.researchgate.net/publication/315837035
[34] Ozdogan-Dolcek, A. (2015). Numerical Modeling of Heat Transport for Ground-Coupled Heat Pump (GCHP) Systems and Associated Life Cycle Assessments. The University of Wisconsin - Madison, ProQuest Dissertations Publishing, 2015. 10134219, 195 p.
[35] Li, Mo. (2013). Life Cycle Assessment of Residential Heating and Cooling Systems in Minnesota: A comprehensive analysis on life cycle greenhouse gas (GHG) emissions and cost effectiveness of ground source heat pump (GSHP) systems compared to the conventional gas furnace and air conditioner system. Retrieved from the University of Minnesota Digital Conservancy, http://hdl.handle.net/11299/146449.

[36] Lee, E. J., Kang, E. C., Kim, J. Y., & Kim, Y. H. (2015). A World-wide Life Cycle Cost Analysis Tool of Ground Source Heat Pump System.
[37] Raadal, H. L., Gagnon, L., Modahl, I. S., & Hanssen, O. J. (2011). Life cycle greenhouse gas (GHG) emissions from the generation of wind and hydro power. Renewable and Sustainable Energy Reviews, 15(7), 3417–3422. https://doi.org/10.1016/j.rser.2011.05.001
[38] Desai, M., & Harvey, R. P. (2017). Inventory of U.S. Greenhouse Gas Emissions and Sinks: 1990-2015. Federal Register (Vol. 82). https://doi.org/EPA 430-R-13-001
[39] Kim, J., Hong, T., Chae, M., Koo, C., & Jeong, J. (2015). An environmental and economic assessment for selecting the optimal ground heat exchanger by considering the entering water temperature. Energies, 8(8), 7752–7776. https://doi.org/10.3390/en8087752
[40] TWB, 2018. The World Bank. Retrieved December 12, 2018, from https://data.worldbank.org/indicator/FR.INR.RINR?view=chart
[41] Fredin, P. W. (2009). Air Force Institute of Technology. Security.
[42] Glassley, W., Asquith, A., Lance, T., & Brown, E. (2012). Assessment of California's Low Temperature Geothermal Resources: Geothermal Heat Pump Efficiencies by Region: Evaluation of Geothermal Heat Pump System Use in California. Retrieved from http://www.energy.ca.gov/2014publications/CEC-500-2014-060/CEC-500-2014-060.pdf
[43] Standards, C. A., & Verification, F. (2014). CEC. https://www.energy.ca.gov/title24/2013standards/residential_manual.html